JOURNAL OF MATERIALS SCIENCE 27 (1992) 4667–4677

Tensile strength of unidirectional γ-Al_2O_3 fibre/Al–5 mass % Cu matrix composite at room and high temperatures

SHOJIRO OCHIAI, TADAO ARAIKE, KENJI TOKINORI, KOZO OSAMURA
Department of Metallurgy, Kyoto University, Kyoto 606, Japan

MITSUHISA NAKATANI
Sumitomo Chemicals Co. Ltd, Chuo-ku, Tokyo 103, Japan

KOJI YAMATSUTA
Sumitomo Chemicals Co. Ltd, Tsukuba, Ibaraki 300-32, Japan

The tensile strength of unidirectional γ-alumina fibre-reinforced Al–5 mass % Cu alloy composite prepared by the casting method, increased with increasing temperature, reaching a peak value at about 500 K, and then decreased. The reason for this is discussed from the viewpoints of influence of ductility of the compound layer ($CuAl_2$) adhering to the fibre surface on the strength of the fibre and the influence of the yield stress of the matrix on the strength of the composite, using a simplified model to calculate strain energy release rate of the fibre and the Monte Carlo simulation technique. Two main results were found. At room temperature, the premature fracture of the compound led to formation of a crack, which caused reduction in strength of the fibre and composite. The temperature dependence of strength of the present composite was considered to be controlled by the following competing factors: increase in ductility of the compound with increasing temperature which acts to raise the strength of the fibre and softening of the matrix which acts to reduce the strength of the composite. The reason why the strength of the composite increased with increasing temperature below 500 K, could be attributed to the predominance of the former factor over the latter one. However the reason why the strength of composite decreased with increasing temperature above 500 K could be attributed to the predominance of the latter factor over the former one.

1. Introduction

The γ-alumina fibre-reinforced aluminium matrix composite is known to have high specific elasticity and strength [1, 2]. In order to improve these properties further, addition of copper into the aluminium matrix has been attempted by Abe *et al.* [2], who found the following results. (a) With this addition, high-temperature properties could be improved: the strength of the composite did not change even after exposure for 1000 h at 723 K. The transverse strength was also improved. (b) However, the room-temperature strength of copper-doped composite was rather lower than the strength of non-doped one. (c) An interesting temperature dependence of strength was found: the strength of composite increased, reaching a peak value at about 500 K and then decreased.

The aim of the present work was to confirm the temperature dependence of strength of this composite and to discuss the reasons why such a reduction at room temperature was caused by copper addition and why such a temperature dependence of strength appeared.

2. Experimental procedure

The γ-alumina fibres of 17 μm average diameter with a chemical composition of 85 wt % Al_2O_3 and 15 wt % SiO_2, were consolidated with Al-5 mass % Cu alloy at Sumitomo Chemical Company by a casting method [1, 2]. The distribution of elemental copper in the composite was observed using an electron probe micro-analyser (EPMA).

The tensile strength of the composite was measured at room temperature, 473 and 673 K in air with an Instron-type tensile machine at a crosshead speed of 8.3×10^{-3} mm s^{-1} using the samples shown in Fig. 1. As shown later, $CuAl_2$ compound was formed on fibre surface. In order to ascertain the influence of the existence of the compound on fibre strength, the fibres were extracted by etching away the matrix with 1% and 10% NaOH solutions. With 1% NaOH solution, the compound was retained on fibre surface, as shown in Fig. 2a, while for 10% solution, it was completely removed from the fibre surface, as shown in Fig. 2b. For comparison, the fibres were also extracted with 1% NaOH solution from the pure aluminium matrix

0022–2461

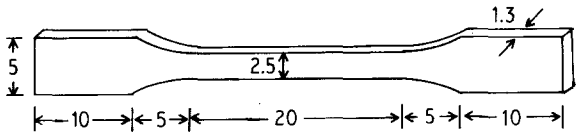

Figure 1 Configuration of samples for the tensile test. Dimensions in mm.

composite. Tensile tests were carried out for the extracted fibres at room temperature at the same crosshead speed for a gauge length of 30 mm.

The fracture surfaces of composite samples and extracted fibres were observed with a scanning electron microscope.

3. Results

3.1. Structure of copper-doped composite

Fig. 3 shows the distribution of elemental copper in the transverse cross-section of the composite. The copper-enriched layer formed on the fibre surface was $CuAl_2$ (θ-phase in the aluminium–copper binary diagram [3]). The concentration of elemental copper in the matrix was 2.2 mass %.

3.2. Temperature dependence of the strength of composite

The tensile strengths of undoped and copper-doped composites at room temperature reported by Abe *et al.* [1, 2] were 860 and 590 MPa, respectively. The addition of copper led to a reduction in strength at room temperature. Fig. 4 shows the variation of strength as a function of temperature, where the strength values are normalized with respect to the average strength of the composite at room temperature, $\sigma_{c,RT}$. It was confirmed that the strength of the composite increases, reaching peak at about 500 K and then decreases with increasing temperature.

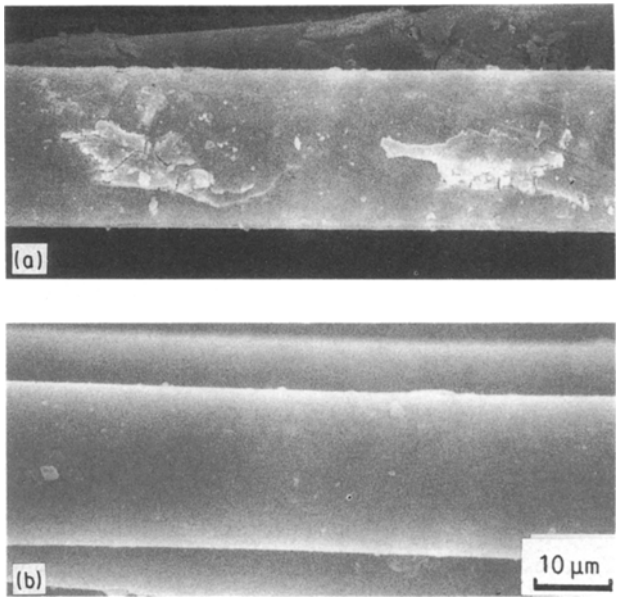

Figure 2 Appearance of side surfaces of the fibres extracted from the composite with (a) 1% and (b) 10% NaOH solutions.

3.3. Fracture morphology

Fig. 5 shows the fracture surfaces of the samples tested at room temperature. It is clearly found that the compound layer ($CuAl_2$) is broken in a brittle manner and the breakage of the fibres is initiated from the compound. In the composite systems of boron (fibre)/aluminium(matrix) [4–6], graphite/aluminium [7], boron/titanium [4] and α-alumina/Al–Li [8], the interfacial reaction layers, covering the side surface of the fibres continuously, are broken during an early

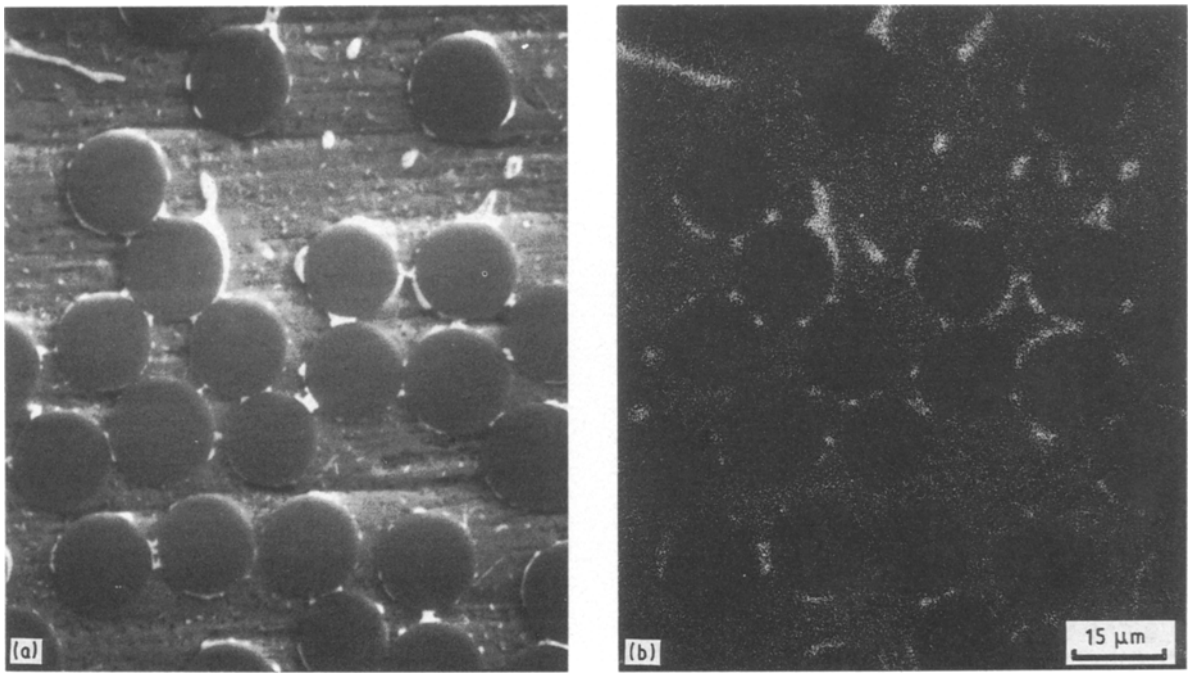

Figure 3 Distribution of elemental copper.

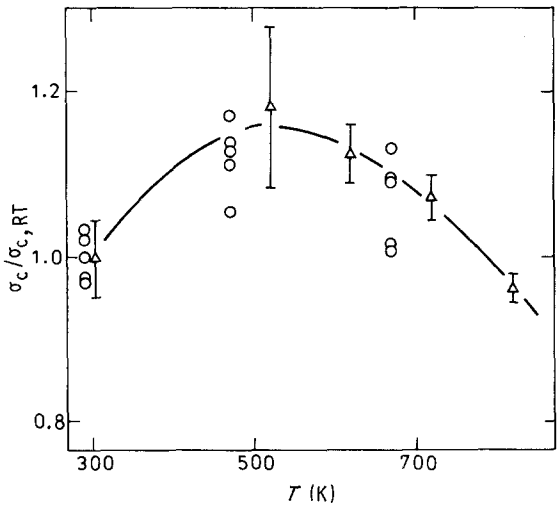

Figure 4 Temperature dependence of strength of the composite samples. The strength, σ_c, is normalized with respect to the strength at room temperature, $\sigma_{c,RT}$. (○) Present work, (△) Abe *et al.* [1, 2].

stage of deformation, making circumferential cracks on the fibre surfaces, which reduces the strength of the fibres. Similar to the strength of these composite systems, the strength of the present composite is considered to be reduced by the premature cracking of the brittle compound layer although the compound is not continuous but almost platelet shaped in the present samples.

Fig. 6 shows the macroscopic fracture morphology of the samples tested at room temperature and 673 K. A typical feature is that the pull-out of fibres becomes predominant at high temperatures.

3.4. Tensile strength of the extracted fibre

Fig. 7 shows the distribution of strength of extracted fibres. Fig. 7a–c refer to the fibres with the compound layer extracted from the copper-doped matrix composite (A), that of the fibres without a compound layer

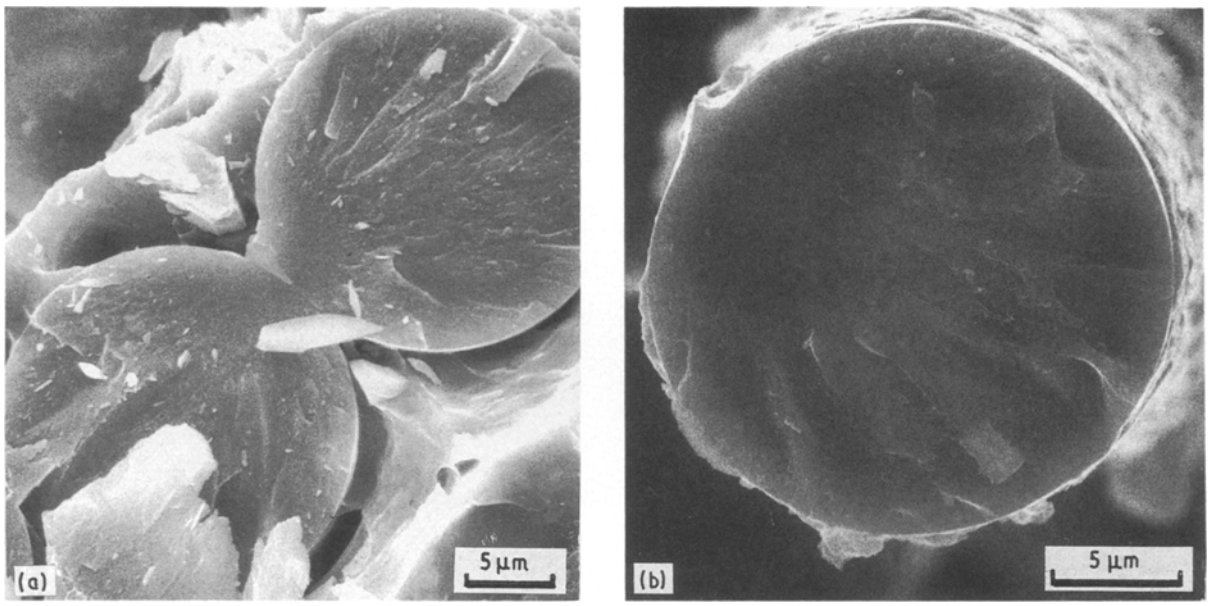

Figure 5 Fracture morphology of fibres in a composite tested at room temperature.

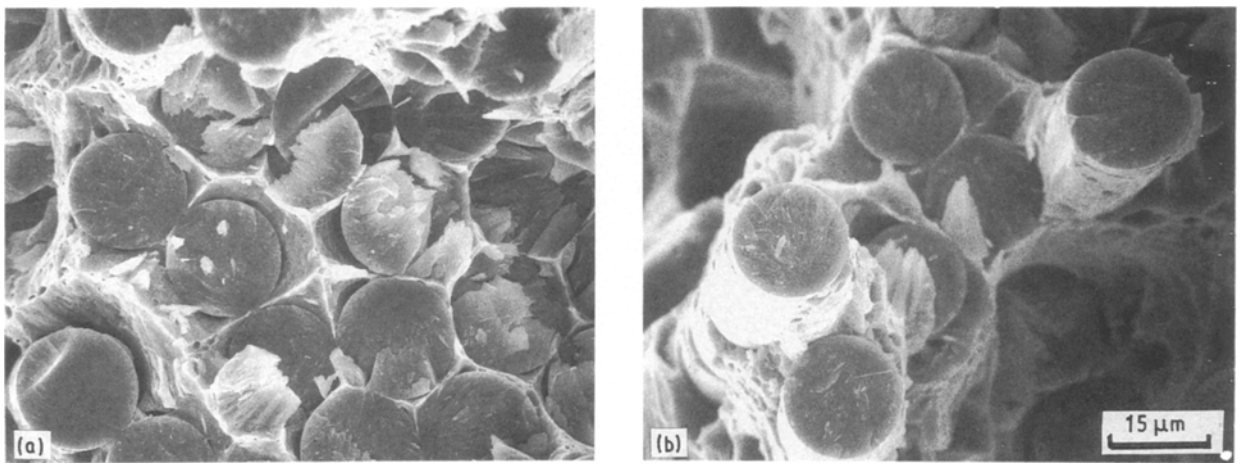

Figure 6 Fracture surface of composite samples tested at (a) room temperature, and (b) 673 K.

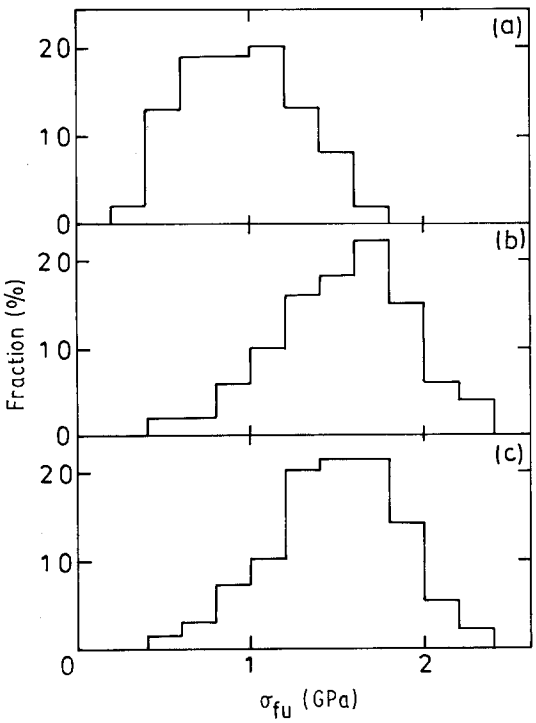

Figure 7 Distribution of strength of fibres A–C extracted from composites. (a) Fibre A, extracted from copper-doped matrix composite with 1% NaOH solution, having the compound on the surfaces. (b) Fibre B, extracted from copper-doped matrix composite with 10% NaOH solution, having no compound on the surfaces. (c) Fibre C, extracted from pure aluminium matrix composite with 1% NaOH solution.

extracted from the copper-doped matrix composite (B), and that of the fibres extracted from the pure aluminium matrix composite (C), respectively. Fig. 8 shows the Weibull plot [9] for fibres A–C. From Figs 7 and 8, the following features could be seen.

1. The strength of the fibres without compound layer (B, 1.6 GPa on an average) was essentially the same as that of the fibres extracted from pure aluminium matrix composite (C, 1.6 GPa), but the strength of the fibres with the compound layer (A, 1.0 GPa) was lower than that of the fibres without a compound layer (B, C).

2. The shape parameters for the Weibull distribution for fibres A–C were 3.0, 4.2 and 4.8, respectively; namely, the scatter of strength of the fibres with a compound layer (A) was large in comparison with that of the fibres without a compound layer (B, C). The strength and shape parameter of bare γ-alumina fibre

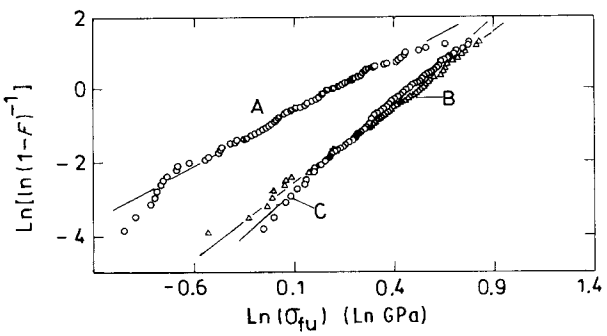

Figure 8 Weibull-plot for fibres A–C. F is the cumulative distribution function.

for gauge length 20 mm have been reported to be 1.8 GPa and 5, respectively, by Abe *et al.* [1, 2]. Applying the length dependence of strength based on the Weibull distribution, the strengths of fibres B and C for the present gauge length, 30 mm, are expected to be 1.8 and 1.7 GPa, respectively, for a gauge length of 20 mm. The strength of the present fibres B and C is essentially the same as that of original one.

From the results stated above, it could be suggested that the copper addition did not degrade the strength of the fibres directly but it degraded the strength through the existence of the compound layer, whose premature fracture resulted in the formation of cracks on the fibre surfaces.

4. Results and discussion

4.1. Reduction in strength of fibres and composite due to copper addition at room temperature

In order to demonstrate numerically how the fibre strength is reduced by the premature fracture of the compound, the strength of the fibre was calculated using the following simplified method. The compound was treated as a platelet in the calculation.

4.1.1. Calculation of the strength of a fibre with a cracked compound layer

Fig. 9 shows a schematic drawing of the model consisting of a single fibre with a strongly adhering compound which is cracked at $Y = 0$ where Y is defined as the distance in the longitudinal direction from the crack. The thickness, width, length and cross-sectional area of the compound are a, W, L and S ($= aW$), respectively. Denoting the applied load as P and the compliance for the notched area S as $C(S)$, the strain energy release rate of the fibre, λ, is given by [10]

$$\lambda = (P^2/2)[dC(S)/dS] \quad (1)$$

where dS is the increment of cross-sectional area of the crack. In this work, λ was calculated by modifying

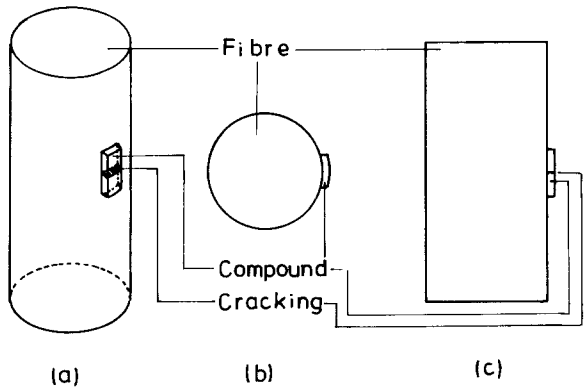

Figure 9 (a) Schematic representation of the fibre with adhering broken compound. (b) Transverse cross-section of the region in which the compound adheres. The compound is shown at the right-hand side. (c) Longitudinal cross-section including compound.

Equation 1 into the form

$$\lambda = (P^2/2)\left\{\lim_{\Delta S \to 0} [C(S + \Delta S) - C(S)]/(\Delta S)\right\} \quad (2)$$

$C(S)$ and $C(S + \Delta S)$ were calculated using the shear-lag-analysis technique [11–14] which has been applied to calculate stress concentrations in the fibres adjacent to broken fibres in fibre-reinforced composites. Fracture of the fibre was regarded to occur when

$$\lambda \geqslant \lambda_c \quad (3)$$

where λ_c is the critical strain energy release rate.

The details of the procedure for calculation are shown in the Appendix.

4.1.2. *Variation of strength of fibre as a function of thickness, length and width of the compound at room temperature*

As the compound layer behaves elastically at room temperature, the calculation was carried out for the situation shown in Fig. A2a in the Appendix.

First, in order to determine the influence of thickness, a, length, L, and width, W, of the compound on the strength of the fibre, calculation was carried out for various combinations of the values of W, L and a for an assumed value of $\lambda_c = 3\ \mathrm{J\,m^{-2}}$. The values of E_f and E_c were taken to be 210 [1, 2] and 130 GPa [15], respectively. The R_f was 8.5 μm [1, 2]. The shear modulus, G, was calculated from $G = E/[2(1 + \nu)]$ where ν is Poisson's ratio, which was taken to be 0.25 in this work.

Figs 10 and 11 show the calculation results on variations of σ_{fu} as a function of W for fixed values of a and L and as a function of a for fixed values of W and L, respectively. The results demonstrate well that the larger the width, W, the length, L, and the thickness, a, of the compound, the lower becomes the strength of fibre.

Denoting the strength of a bare fibre as σ_{fu}^0, the strength of the fibre is given by σ_{fu}^0 if the width of the compound is narrower than a critical value, W_{crit}, for fixed values of L and a, because the crack cannot extend into the fibre because $\lambda < \lambda_c$ for $W < W_{crit}$. In this range, the calculated values of σ_{fu} are higher than σ_{fu}^0, which means that the fibre is broken due to its intrinsic defects. Taking $\sigma_{fu}^0 = 1.8$ GPa as an example, the strength of fibre varies, for instance, along ABC as a function of W for fixed values of $a = 0.5$ μm and $L = 2$ μm, as shown in Fig. 10. The critical value of W_{crit} is dependent on the values of a and L: it becomes large when the values of L and a are small, while it becomes small when those are large. In a similar manner, there are critical length L_{crit} and critical thickness a_{crit}, below which no reduction in fibre strength occurs, for fixed values of a and W and for those of W and L, respectively. These critical values become small when other parameters become large, as well as W_{crit}.

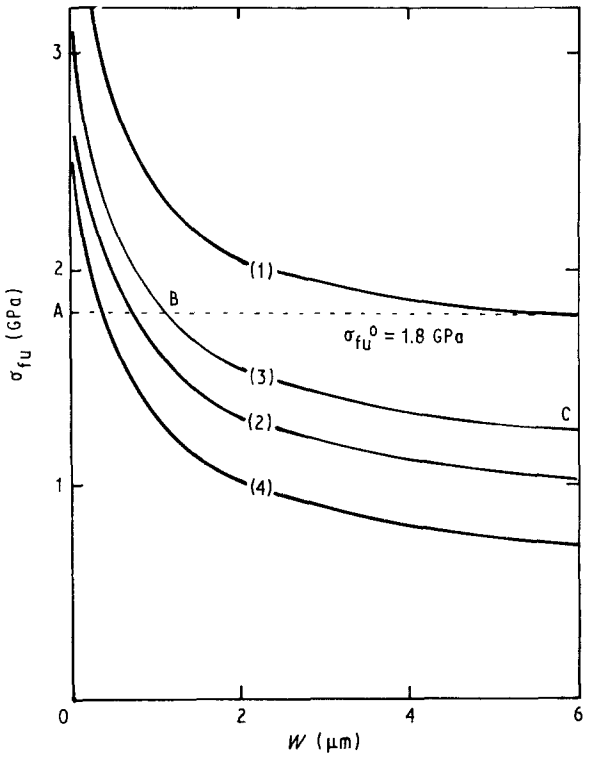

Figure 10 Influence of width, W, of the compound on the strength of the fibre, σ_{fu}, for a fixed length, L, and thickness, a, of compound. $\lambda_c = 3\ \mathrm{J\,m^{-3}}$. (1) $a = 0.5$ μm, $L = 2$ μm; (2) $a = 0.5$ μm, $L = 10$ μm; (3) $a = 2.0$ μm, $L = 2$ μm; (4) $a = 2.0$ μm, $L = 10$ μm.

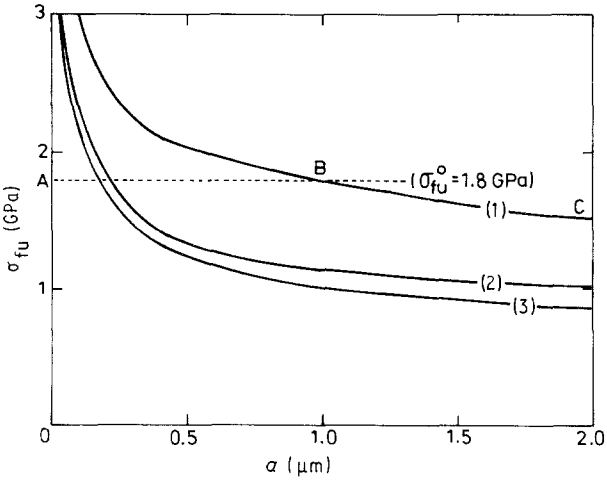

Figure 11 Influence of thickness, a, of a compound on strength of a fibre, σ_{fu}, for a fixed width, W, and length, L, of compound. $\lambda_c = 3\ \mathrm{J\,m^{-2}}$. (1) $W = 2$ μm, $L = 2$ μm; (2) $W = 2$ μm, $L = 10$ μm; (3) $W = 5$ μm, $L = 10$ μm.

From the calculation, it is well understood that the premature fracture of the compound layer reduces the strength of fibres when the size of the compound is large. The difference in strength between an aluminium matrix composite (860 MPa) and a copper-doped aluminium matrix one (590 MPa) could be understood in this way.

4.2. Temperature dependence of the strength of a composite

As shown in Fig. 4, the strength of the composite increased with increasing temperature and then decreased. Furthermore, the strength below about

700 K was higher than the strength at room temperature. Why such a temperature dependence appeared could be explained as follows from the viewpoints of plasticity of the compound and the yield stress of the matrix.

4.2.1. Influence of plasticity of a compound on strength of a fibre

The plasticity of the present compound ($CuAl_2$) was investigated by Herzberg *et al.* [15] who found that the onset temperature was 423 K from the tensile testing of unidirectionally solidified eutectic $CuAl_2$–aluminium composite alloy. If plasticity appears in the compound above 423 K, it will reduce the strain energy release rate and raise the strength of the fibre. To demonstrate this speculation, the strain energy release rate of the fibre, λ, was calculated by the procedure shown in the Appendix. An example of the results of the calculation is shown in Fig. 12 where the shear yield stress of the compound is varied from 100–500 MPa for fixed values of a, W and L. From Fig. 12, the following features could be seen.

1. λ is proportional to the square of the applied stress, σ_f^2 when the applied stress is low. Once yielding occurs at high applied stress, the strain energy release rate becomes lower than the linear relation. This indicates that when the plasticity appears in the compound above 423 K, the strain energy release rate of the fibre becomes small.

2. The lower the yield stress of the compound, the lower the strain energy release rate of the fibre becomes, at high applied stress.

3. If we assume $\lambda_c = 3\ J\ m^{-2}$, the strength of the fibre increases from 0.88 GPa for $\tau_y = 500$ MPa to 1.34 GPa for $\tau_y = 100$ MPa. This indicates that the lower the yield stress of the compound, the higher the strength becomes.

Feature 3 suggests that the strength of the fibre increases with increasing temperature, because the yield stress of the compound decreases with increasing temperature. The reason why the strength of the composite increases with increasing temperature up to about 500 K could be attributed to this effect. On the other hand, why the strength of the composite decreases with increasing temperature beyond about 500 K cannot be explained by this effect, because it predicts only an increase in strength with increasing temperature. In order to explain the reduction above 500 K, the factors which act to reduce strength should be taken into consideration. As one such factor, the softening of the matrix can be mentioned. In the following section, the influence of this factor on the strength of composite is discussed.

4.2.2. Influence of softening of matrix on strength of composite

As the strength of the fibres has a scatter as shown in Fig. 3, weaker fibres will be broken prior to stronger ones. When weaker fibres are broken, a stress concentration arises in the neighbouring fibres together with a loss of load-bearing capacity of the broken fibres within the distance of the half-critical length from the broken ends. The loss of load-bearing capacity of the broken fibres is large when the critical length becomes large [16]. Both stress concentration and critical length are affected by the softening of the matrix.

The stress concentration and critical length can be calculated using the shear-lag-analysis method [13]. Figs 13 and 14 show examples of the variation of stress concentration factor, K, and that of critical length, l_c, as a function of applied stress on the fibres, σ_f, at infinity, for various yield stresses of the matrix τ_{my}. The stress concentration factor decreases but the critical length increases with decreasing yield stress of the matrix. This indicates that softening of the matrix acts to raise the strength of the composite from the point of decrease in stress concentration, but it acts also to reduce the strength from the point of increase in the

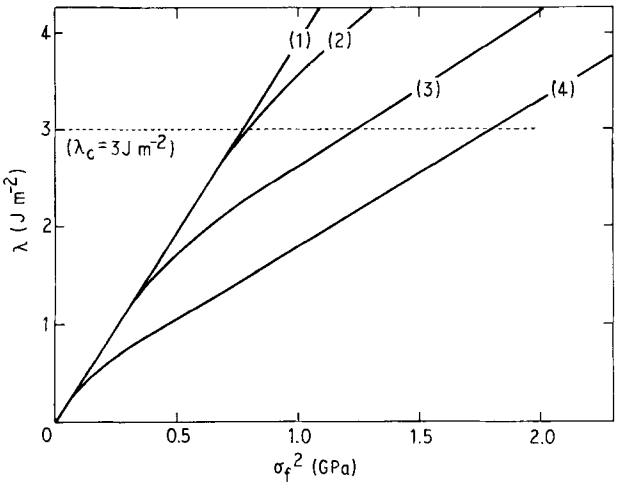

Figure 12 Strain energy release rate of a fibre, λ, plotted against square of fibre stress, σ_f^2, for various yield stresses of the compound at $\lambda_c = 3\ J\ m^{-2}$, for fixed length, $L = 10\ \mu m$, width, $W = 5\ \mu m$, and thickness, $a = 2\ \mu m$. (1) $\tau_y = 500$ MPa, $\sigma_{fu} = 0.88$ GPa; (2) $\tau_y = 300$ MPa, $\sigma_{fu} = 0.89$ GPa; (3) $\tau_y = 200$ MPa, $\sigma_{fu} = 1.11$ GPa; (4) $\tau_y = 100$ MPa, $\sigma_{fu} = 1.34$ GPa.

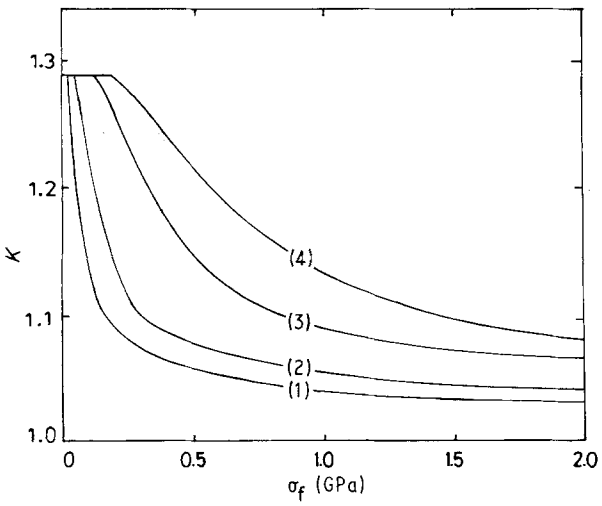

Figure 13 Influence of shear yield stress of matrix, τ_{my}, on the stress concentration factor, K, in the fibres neighbouring a broken fibre. τ_{my}: (1) 5 MPa, (2) 10 MPa, (3) 30 MPa, (4) 50 MPa.

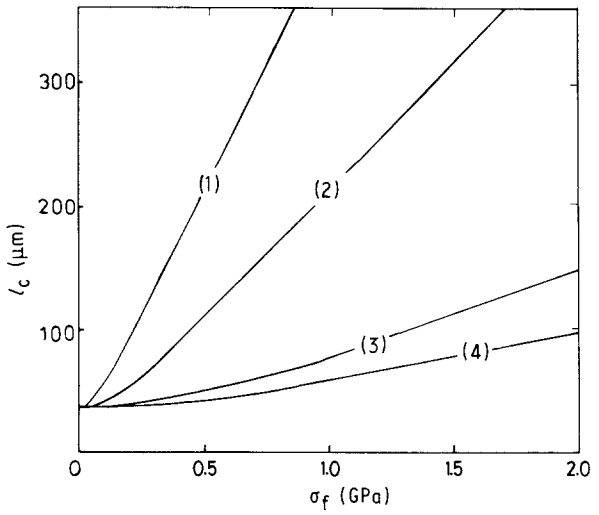

Figure 14 Influence of shear yield stress of a matrix, τ_{my}, on critical length, l_c. τ_τ: (1) 5 MPa, (2) 10 MPa, (3) 30 MPa, (4) 50 MPa.

critical length. Thus the strength of a composite is determined by the competition of these factors.

In the present work, in order to determine how these factors act to determine the strength of a composite as a function of yield stress of the matrix, a Monte-Carlo simulation method was applied. The procedure of this method has been described elsewhere [17]. Fig. 15 shows the results in which the strength of composite, σ_c, is normalized with respect to the prediction based on the rule of mixtures, $\sigma_{c,ROM}$, and the yield stress of the matrix, τ_{my}, is normalized with respect to the average strength of the fibres, σ_{fu}^0. The strength of the composite, σ_c, increases but then decreases with increasing shear yield stress of the matrix. This result indicates that the influence of the decrease in critical length is predominant over that of the increase in stress concentration in the range $\tau_{my}/\sigma_{fu}^0 < 0.05$, resulting in an increase in strength of the composite with increasing yield stress of the matrix, while the latter is predominant over the former in the range $\tau_{my}/\sigma_{fu}^0 > 0.05$, resulting in a reduction in strength with increasing yield stress of the matrix. As $\tau_{my} < 50$ MPa and $\sigma_{fu}^0 = 1.8$ GPa in the present samples, the strength of the composite decreases with decreasing yield stress of matrix, i.e. with increasing temperature.

Summarizing the results of Sections 4.2.1 and 4.2.2, it might be concluded that the strength of the composite increases with increasing temperature due to the appearance of plasticity of the compound, but it decreases at high temperatures due to softening of the matrix although the fibre strength is expected to increase.

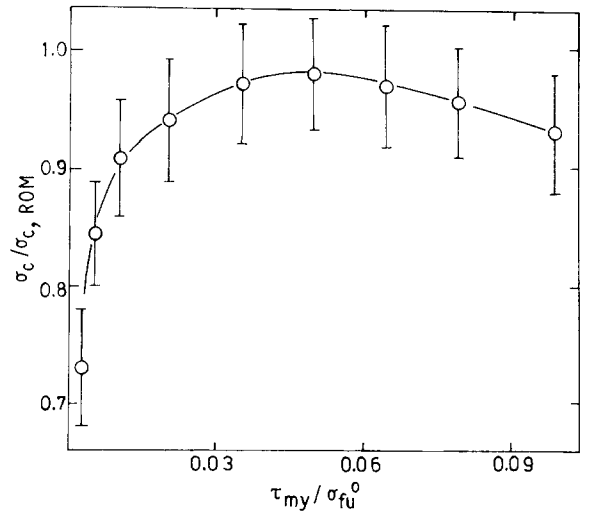

Figure 15 Variation of the strength of a composite, σ_c, as a function of shear yield stress of the matrix, τ_{my}, predicted by a Monte-Carlo computer simulation technique [16]. The strength is normalized with respect to the prediction based on the rule of mixtures and the shear yield stress of the matrix is normalized with respect to the average strength of the fibres, σ_{fu}^0. The Weibull shape parameter is taken to be 5.

5. Conclusions

The reduction in strength of γ-alumina fibre-reinforced aluminium matrix composite at room temperature due to addition of elemental copper into the matrix could be attributed to the formation of a crack on the fibre surface introduced by a premature fracture of adhering compound $CuAl_2$. The strength of the composite increased with increasing temperature due to plasticity of the compound, but then decreased due to softening of the matrix, which led to an increase in critical length, resulting in a loss of load-bearing capacity of the fibres.

Acknowledgements

The authors thank Messrs I. Nakagawa and T. Unesaki, Kyoto University, for their help in the SEM and EPMA studies, and The Ministry of Education, Science and Culture of Japan, for the grant-in-aid (no. 01550549).

Appendix: calculation of the strain energy release rate of a fibre

A1. Modelling

For the calculation, a fibre with a compound layer on its surface was modelled as follows.

The fibre, of radius R_f, cross-sectional area S_f, and length L_f, has a platelet-compound with thickness a, length L and width W, as shown in Fig. A1. Young's and shear moduli of the fibre are E_f and G_f, respectively, and those of the compound E_c and G_c, respectively.

In the present work, for simplicity, the fibre was regarded to be composed of $N1$ platelet elements as shown in Fig. A1. The cross-sectional area of each element was taken to be equal to that of the compound ($= aW$). The element at the left-hand side was numbered 1, the next one 2, and then 3, 4, . . . , and $N1$ to the right-hand side. The compound was numbered N where $N = N1 + 1$. The thickness and width of element i were denoted T_i and W_i, respectively. The interface between elements $i - 1$ and i was expressed as $i - 1/i$ interface. The displacement from $Y = 0$ of element i was denoted U_i and that of the interface between $i - 1$ and i, $U_{i-1/i}$. The Young's and shear

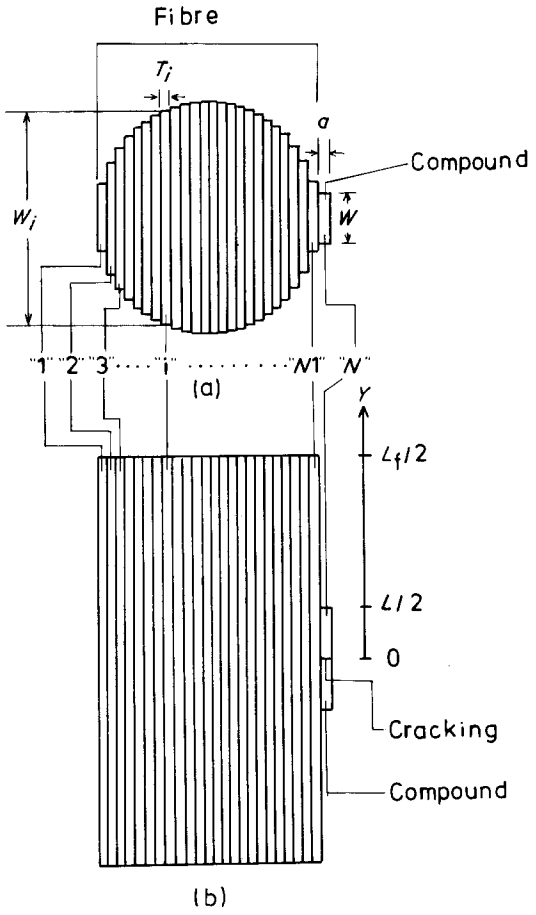

Figure A1 Modelling of a fibre with a cracked compound platelet for application of shear lag analysis. (a) Schematic drawing of a transverse cross-section at $Y = 0$ divided into N elements. (b) Longitudinal cross-section.

moduli of element i were shown by E_i and G_i, respectively. If element i existed within the fibre, E_i and G_i were given by E_f and G_f, respectively, while, if it existed within the compound, they were given by E_c and G_c, respectively.

A2. Definition of regions

The compound layer deforms elastically at room temperature. On the other hand, plasticity appears in the compound above 423 K [15]. In the present calculation, for the room-temperature strength of a fibre with a compound layer, the critical strain energy release rate of the fibre was calculated based on the elastic deformation of fibre and compound and on the elastic stress transfer at the fibre–compound interface. On the other hand, the shear yielding at the interface was taken into consideration for the strength above 423 K. This calculation method is rough, because tensile yielding of the compound at high temperatures is ignored. However, even this rough calculation can show the reduction in strain energy release rate of the fibre, as shown in Section 4.2.

At the interface between the fibre and compound, shear stress arises. When the exerted shear stress becomes higher than the shear yield stress of the compound, the compound at the interface deforms plastically in shear.

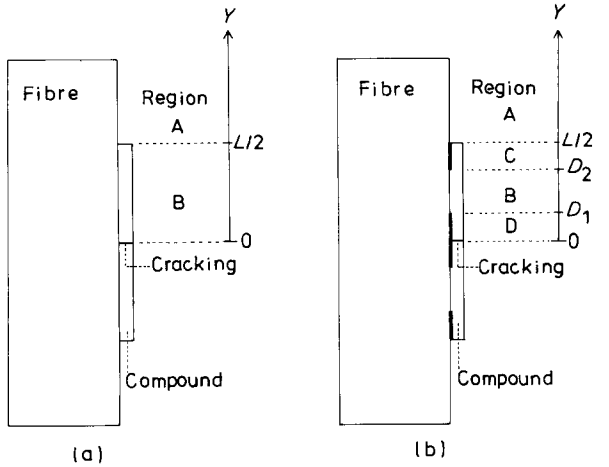

Figure A2 Schematic representation of regions which appear (a) when the compound has no plasticity, and (b) when it has plasticity. In (b), the compound at the interface deforms plastically in shear in Regions C and D, but elastically in Region B.

At room temperature, as the compound deforms elastically, there are two regions, as schematically shown in Fig. A2a: Region A ($Y \geqslant L/2$) where no compound adheres to the fibre (i.e. bare fibre region) and Region B ($0 \leqslant Y \leqslant L/2$) where the compound adheres and deforms elastically at the interface.

On the other hand, above 423 K, shear yielding occurs in the compound at the interface. As highest shear stress is exerted at the cracking portion ($Y = 0$) and the next highest one at the compound ends ($Y = L/2$), the shear yielding of the compound occurs first at $Y = 0$ and then $L/2$. The yielding regions grow with increasing applied stress. Now we define the yielding regions as Regions C and D and the lengths of the former and latter regions as $L/2 - D_2$ and D_1, respectively, as shown in Fig. A2b. In this case, there are four regions: Regions A ($Y \geqslant L/2$), B ($D_1 \leqslant Y \leqslant D_2$), C ($D_2 \leqslant Y \leqslant L/2$) and D ($0 \leqslant Y \leqslant D_1$).

A3. Equations for stress equilibrium

For Regions A and B, applying Dow's expression [14] which was originally proposed to calculate stress transfer from matrix to fibre in a fibre-reinforced composite, the interfacial shear stress at the $i/i+1$ interface, $\tau_{i/i+1}$, is approximately written as

$$\tau_{i/i+1} = G_i(U_{i/i+1} - U_i)/(T_i/2)$$
$$= G_{i+1}(U_{i+1} - U_{i/i+1})/(T_{i+1}/2) \quad \text{(A1)}$$

Eliminating $U_{i/i+1}$ in Equation A1, we have

$$\tau_{i/i+1} = H_i(U_{i+1} - U_i) \quad \text{(A2)}$$

$$H_i = 2G_iG_{i+1}/(G_iT_{i+1} + G_{i+1}T_i) \quad \text{(A3)}$$

($i = 1$ to $N1 - 1$ for Region A and 1 to $N - 1$ for Region B).

For Regions C and D, the shear stress for $i = 1$ to $N1 - 1$ is also given by Equation A2, and the shear stress $\tau_{N1/N}$ is given by the shear yield stress of the compound, τ_y.

Denoting the cross-sectional area of element i as S_i and the length of interface between elements i and

$i + 1$, which is given by the smaller value between W_i and W_{i+1}, as Q_i, the equations for stress equilibrium are given as follows.

Region A

$$S_1E_1(d^2U_1/dY^2) + Q_1\tau_{1/2} = 0 \quad (A4)$$

$$S_iE_i(d^2U_i/dY^2) + Q_i\tau_{i/i+1} - Q_{i-1}\tau_{i-1/i} = 0 \quad (i = 1 \text{ to } N1 - 1) \quad (A5)$$

$$S_NE_N(d^2U_N1/dY^2) - Q_{N1-1}\tau_{N1-1/N1} = 0 \quad (A6)$$

Region B

$$S_1E_1(d^2U_1/dY^2) + Q_1\tau_{1/2} = 0 \quad (A7)$$

$$S_iE_i(d^2U_i/dY^2) + Q_i\tau_{i/i+1} - Q_{i-1}\tau_{i-1/i} = 0 \quad (i = 1 \text{ to } N - 1) \quad (A8)$$

$$S_NE_N(d^2U_N/dY^2) - Q_{N-1}\tau_{N-1/N} = 0 \quad (A9)$$

Regions C and D

$$S_1E_1(d^2U_1/dY^2) + Q_1\tau_{1/2} = 0 \quad (A10)$$

$$S_iE_i(d^2U_i/dY^2) + Q_i\tau_{i/i+1} - Q_{i-1}\tau_{i-1/i} = 0 \quad (i = 1 \text{ to } N1 - 1) \quad (A11)$$

$$S_{N1}E_{N1}(d^2U_{N1}/dY^2) + Q_{N1}\tau_y - Q_{N1-1}\tau_{N1-1/N1} = 0 \quad (A12)$$

$$S_NE_N(d^2U_N/dY^2) - Q_{N-1}\tau_y = 0 \quad (A13)$$

A4. Non-dimensionalization

In order to obtain a convenient form for the problem, non-dimensionalization has been done in the shear lag analysis [11–13]. In this work, the ordinary expression of non-dimensionalization was modified for the present problem as follows.

$$T_i = T_1t_i \quad (A14)$$

$$W_i = T_1w_i \quad (A15)$$

$$S_i = S_1s_i = W_1T_1s_i = T_1^2w_1s_i \quad (A16)$$

$$E_i = E_1e_i \quad (A17)$$

$$G_i = G_1g_i \quad (A18)$$

$$H_i = G_1h_i/T_1 \quad [h_i = 2g_ig_{i+1}/(g_it_{i+1} + g_{i+1}t_i)] \quad (A19)$$

$$U_i(i = 1 \text{ to } N) = \sigma_f T_1[1/(E_1G_1)]^{1/2}u_i \quad (A20)$$

$$Q_i = T_iq_i(q_i = w_i \text{ when } w_i < w_{i-1} \text{ and } q_i = w_{i+1} \text{ when } w_i > w_{i+1}) \quad (A21)$$

$$Y = T_1(E_1/G_1)^{1/2}y \quad (A22)$$

$$L = T_1(E_1/G_1)^{1/2}l \quad (A23)$$

$$L_f = T_1(E_1/G_1)^{1/2}l_f \quad (A24)$$

$$D_1 = T_1(E_1/G_1)^{1/2}d_1 \quad (A25)$$

$$D_2 = T_1(E_1/G_1)^{1/2}d_2 \quad (A26)$$

$$\tau_y = \sigma_f(G_1/E_1)^{1/2}\tau_y' \quad (A27)$$

where σ_f is the fibre stress at infinity ($Y = \infty$). The t_i, w_i, s_i, e_i, g_i, h_i, u_i, q_i, y, l, l_f, d_1, d_2 and τ_y' are non-dimensionalized forms of T_i, W_i, S_i, E_i, G_i, H_i, U_i, Q_i, Y, L, L_f, D_1, D_2 and τ_y, respectively. Under this non-dimensionalization, the stress concentration factor, K_i, is given by

$$K_i = du_i/dy \quad (A28)$$

Substituting Equations A14–A27 into Equations A4–A13 and letting

$$2q_ih_i/(e_is_i) = m_i \quad (A29)$$

$$2q_{i-1}h_{i-1}/(e_is_i) = n_i \quad (A30)$$

we have following simplified equations:

Region A

$$d^2u_1/dy^2 + m_1(u_2 - u_1) = 0 \quad (A31)$$

$$d^2u_i/dy^2 + m_iu_{i+1} - (m_i + n_i)u_i + n_iu_{i-1} = 0 \quad (i = 1 \text{ to } N1 - 1) \quad (A32)$$

$$d^2u_N/dy^2 - n_{N1}(u_{N1} - u_{N1-1}) \quad (A33)$$

Region B

$$d^2u_1/dy^2 + m_1(u_2 - u_1) = 0 \quad (A34)$$

$$d^2u_i/dy^2 + m_iu_{i+1} - (m_i + n_i)u_i + n_iu_{i-1} = 0 \quad (i = 1 \text{ to } N - 1) \quad (A35)$$

$$d^2u_N/dy^2 - n_N(u_N - u_{N-1}) \quad (A36)$$

Regions C and D

$$d^2u_1/dy^2 + m_1(u_2 - u_1) = 0 \quad (A37)$$

$$d^2u_i/dy^2 + m_iu_{i+1} - (m_i + n_i)u_i + n_iu_{i-1} = 0 \quad (i = 1 \text{ to } N1 - 1) \quad (A38)$$

$$d^2u_{N1}/dy^2 + [w_{N1}/(e_{N1}s_{N1})]\tau_y' - n_{N1}(u_{N1} - u_{N1-1}) = 0 \quad (A39)$$

$$d^2u_N/dy^2 - [w_N/(e_Ns_N)]\tau_y' = 0 \quad (A40)$$

A5. General solution of u_i

The general solutions of u_i ($i = 1$–$N1$ for Region A and $i = 1$–N for Regions B–D) are given as follows under a condition of $K = 1$ at infinity ($Y = \infty$).

Region A

$$u_i^A = \sum_{j=1}^{N_1-1} A_jB_{i,j}\exp(-k_jy) + y + A_{N1} \quad (A41)$$

where A_j are unknown constants, $(k_j)^2$ ($k_j > 0$) are eigen values except zero for the matrix T_{N1} given by

$$T_{N1} = \begin{bmatrix} m_1 & -m_1 & & & & \\ -n_2 & m_2+n_2 & -m_2 & & 0 & \\ & -n_3 & m_3+n_3 & -m_3 & & \\ \cdots & \cdots & \cdots & \cdots & \cdots & \cdots \\ & 0 & & -n_{N1-1} & m_{N1-1}+n_{N1-1} & -m_{N1-1} \\ & & & & -n_{N1} & n_{N1} \end{bmatrix} \quad \text{(A42)}$$

and $B_{i,j}$ are constants given by

$$B_{1,j} = 1 \quad (j = 1 \text{ to } N1 - 1) \quad \text{(A43)}$$

$$B_{2,j} = (1 - k_j^2/m_1)B_{1,j} \quad (j = 1 \text{ to } N1 - 1) \quad \text{(A44)}$$

$$B_{i,j} = (1 + n_{i-1}/m_{i-1} - k_j^2/m_{i-1})B_{i-1,j} - (n_{i-1}/m_{i-1})B_{i-2,j} \quad (i = 3 \text{ to } N1, \quad j = 1 \text{ to } N1 - 1) \quad \text{(A45)}$$

Region B

$$u_i^B = \sum_{j=1}^{2(N-1)} C_j D_{i,j} \exp(v_j y) + C_{2N-1} y + C_{2N} \quad \text{(A46)}$$

where C_j are unknown constants, $(v_j)^2$ are eigen values except zero for the matrix T_N given by

$$T_N = \begin{bmatrix} m_1 & -m_1 & & & & \\ -n_2 & m_2+n_2 & -m_2 & & 0 & \\ & -n_3 & m_3+n_3 & -m_3 & & \\ \cdots & \cdots & \cdots & \cdots & \cdots & \cdots \\ & 0 & & -n_{N-1} & m_{N-1}+n_{N-1} & -m_{N-1} \\ & & & & -n_N & n_N \end{bmatrix} \quad \text{(A47)}$$

and $D_{i,j}$ are constants given by

$$D_{1,j} = 1 \quad (j = 1 \text{ to } 2(N-1)) \quad \text{(A48)}$$

$$D_{2,j} = (1 - k_j^2/m_1)B_{1,j} \quad (j = 1 \text{ to } 2(N1 - 1)) \quad \text{(A49)}$$

$$D_{i,j} = (1 + n_{i-1}/m_{i-1} - k_j^2/m_{i-1})B_{i-1,j} - (n_{i-1}/m_{i-1})B_{i-2,j} \quad (i = 3 \text{ to } N, \quad j = 1 \text{ to } 2(N-1)) \quad \text{(A50)}$$

Region C

$$u_i^C = \sum_{j=1}^{2(N1-1)} P_j B_{i,j} \exp(k_j y) + P_{2N1-1} y + P_{2N1} + (w_{N1}\tau'_y/\{e_{N1}s_{N1}[1 - n_{N1}L_1(N1)]\}) \times [y^2/2 + L_2(i)] \quad (i = 1 \text{ to } N1) \quad \text{(A51)}$$

$$u_N^C = -w_N\tau'_y y^2/(2e_N s_N) + P_{2N1+1} + P_{2N} \quad \text{(A52)}$$

where P_i ($i = 1$–$2N$) are unknown values, k_{j+N1-1} is equal to $-k_j$ for $i = 1$–$N1 - 1$ where $(k_j)^2$ ($k_j > 0$) are eigen values given by Equation A42 and $L_1(i)$ and $L_2(i)$ are given by

$$L_1(1) = 0 \quad \text{(A53)}$$

$$L_1(2) = -1/m_1 \quad \text{(A54)}$$

$$L_1(i) = -1/m_{i-1} + n_{i-1}L_1(i-1)/m_{i-1} \quad (i = 3 \text{ to } N1) \quad \text{(A55)}$$

$$L_2(1) = 0 \quad \text{(A56)}$$

$$L_2(2) = -1/m_1 \quad \text{(A57)}$$

$$L_2(i) = L_2(i-1) + L_1(i) \quad (i = 3 \text{ to } N1) \quad \text{(A58)}$$

Region D

$$u_i^C = \sum_{j=1}^{2(N1-1)} R_j B_{i,j} \exp(k_j y) + R_{2N1-1} y + R_{2N1} + (w_{N1}\tau'_y/\{e_{N1}s_{N1}[1 - n_{N1}L_1(N_1)]\}) \times [y^2/2 + L_2(i)] \quad (i = 1 \text{ to } N1) \quad \text{(A59)}$$

$$u_N^C = -w_N\tau'_y y^2/(2e_N s_N) + R_{2N1+1} + R_{2N} \quad \text{(A60)}$$

where R_i ($i = 1$–$2N$) are unknown values.

A6. Boundary conditions

The unknown constants, A_j ($j = 1$–$N1$) and C_j, P_j, R_j ($j = 1$–$2N$), d_1 and d_2 could be solved from the following boundary conditions when Regions A–D exist. When only Regions A and B exist, the boundary conditions 2 given below were removed.

A6.1. Case A: no fibre-elements are broken

1. At $y = 0$, the displacements of fibre-elements (1–N_1) are zero, and the stress of compound-element (N) is zero.

2. At $y = d_1$ and d_2, the stresses and displacements of all elements are continuous, and the shear stresses at the fibre–compound interface are equal to the shear yield stress of the compound.

3. At $y = 1/2$, the stresses and displacements of fibre-elements are continuous, and the stress of the compound-elements is zero.

A6.2. Case B: the fibre-element N1 is broken

The boundary conditions 2 and 3 are the same as above. Condition 1 was modified as follows.

1′. At $y = 0$, the displacements of fibre-elements (1–$N1 - 1$) are zero, and stresses of fibre-element ($N1$) and compound element (N) are zero.

A6.3. Case C: the fibre-elements N1 − 1 and N1 are broken

The boundary conditions 2 and 3 are the same as above. Condition 1 was modified as follows.

1″. At $y = 0$, the displacements of fibre-elements (1–$N1 - 2$) are zero, and the stresses of fibre-elements ($N1 - 1$ and $N1$) and compound-element (N) are zero.

A7. Strain energy release rate, λ

Assuming that L_f is large, $\exp(-k_j l_f/2)$ in Equation A41 is nearly zero, where l_f is a non-dimensional form of L_f given by Equation A24. In such a situation, the displacements of all fibre-elements at $Y = L_f/2$ is given by $l_f/2 + A_{N1}$ in non-dimensional form. Noting the displacement at $Y = L_f/2$ for crack area S as $U(S)$ and the value of A_{N1} for crack area S as $A_{N1}(S)$, $U(S)$ is expressed as

$$U(S) = L_f/2 + A_{N1}(S) \quad \text{(A61)}$$

The compliance for crack area S, $C(S)$, is then given by

$$\begin{aligned} C(S) &= 2U(S)/P \\ &= [L_f + 2A_{N1}(S)]/P \end{aligned} \quad \text{(A62)}$$

where P is the applied load. Now let the crack propagate by ΔS. Noting the displacement of all elements at $Y = L_f/2$ for crack area $S + \Delta S$ as $U(S + \Delta S)$ and the value of A_{N1} as $A_{N1}(S + \Delta S)$, the compliance $C(S + \Delta S)$ is given by

$$\begin{aligned} C(S + \Delta S) &= 2U(S + \Delta S)/P \\ &= [L_f + 2A_{N1}(S + \Delta S)]/P \end{aligned} \quad \text{(A63)}$$

P is given by $\pi R_f^2 \sigma_f$. Combining Equations A20, A62 and A63 with Equation 2, we have

$$\lambda = (\pi R_f^2 \sigma_f^2)[1/(E_f G_f)]^{1/2} \left(\lim_{\Delta S \to 0} T_1 \{[A_{N1}(S + \Delta S) - A_{N1}(S)]/\Delta S\} \right) \quad \text{(A64)}$$

In the present work, λ was calculated as follows. $A_{N1}(S)$ was calculated by using the boundary conditions for Case A. Next, ΔS (described as ΔS_1) was taken to be the cross-sectional area of $N1$ element ($\Delta S_1 = S_{N1}$), and the unknown constant $A_{N1}(S + \Delta S_1)$ was obtained by using the boundary conditions for Case B. Then $\Delta S(\Delta S_2)$ were taken to be the sum of the cross-sectional area of $N_1 - 1$ and N_1 elements and the unknown constant $A_{N1}(S + \Delta S_2)$ was obtained by using the boundary conditions for Case C. The value of λ was obtained by linear extrapolation to $\Delta S = 0$.

References

1. Y. ABE, S. HORIKIRI, K. FUJIMURA and E. ICHISE, in "Progress in Science and Engineering of Composites", edited by T. Hayashi, K. Kawata and S. Umekawa (Japan Society of Composite Materials, Tokyo, 1982) pp. 1427–37.
2. Y. ABE, M. NAKATANI, K. YAMATSUTA and S. HORIKIRI, in "Proceedings of the 1st European Conference on Composite Materials", Bordeaux, (European Association for Composite Materials, 1985) pp. 604–9.
3. M. HANSEN (ed.), "Constitution of Binary Alloys" (McGraw-Hill, New York, 1958) pp. 84–90.
4. A. G. METCALFE and M. J. KLEIN, in "Interfaces in Metal-Matrix Composites", edited by A. G. Metcalfe, (Academic Press, New York, 1974) pp. 125–68.
5. J. A. DICARLO, in "Proceedings, Mechanical Behaviour of Metal/Matrix Composites" edited by J. E. Hack and M. F. Amateau (AIME, Pennsylvania, 1983) pp. 1–14.
6. S. OCHIAI, K. OSAMURA and Y. MURAKAMI, in "Progress in Science and Engineering of Composites", edited by T. Hayashi, K. Kawata and S. Umekawa (Japan Society of Composite Materials, Tokyo, 1982) pp. 1331–8.
7. I. H. KHAN, *Metall. Trans.* **7A** (1976) 1281.
8. W. H. HUNT Jr, in "Interfaces in Metal-Matrix Composites", edited by A. K. Dhingra and S. G. Fishman (The Metallurgical Society, PA, 1986) pp. 3–25.
9. W. WEIBULL, *J. Appl. Mech.* **18** (1951) 293.
10. H. TADA, P. C. PARIS and G. R. IRWIN, in "The Stress Analysis Hand Book" (Del Research Corporation, Hellertown, PA, 1973), pp. 1–31.
11. J. M. HEDGEPETH, NASA TN D-882 (1961).
12. J. A. NARIN, *J. Compos. Mater.* **22** (1988) 561.
13. S. OCHIAI and K. OSAMURA, *J. Mater. Sci.* **24** (1989) 3865.
14. N. F. DOW, GEC Missile and Space Division, Report No. R63SD61, quoted by G. S. Holister and C. Thomas in "Fiber Reinforced Materials" (Elsevier, London, 1966) p. 23.
15. R. W. HERZBERG, F. D. LEMKEY and J. A. FORD, *Trans. TMS AIME* **233** (1965) 342.
16. S. OCHIAI and K. OSAMURA, *J. Mater. Sci.* **23** (1988) 886.
17. *Idem, Tetsu-to-Hagane* **75** (1989) 1730 (in Japanese).

Received 29 April
and accepted 2 August 1991